Special Issue

Normative Data for Vascular Density in Superficial and Deep Capillary Plexuses of Healthy Adults Assessed by Optical Coherence Tomography Angiography

Florence Coscas,[1] Alexandre Sellam,[1] Agnès Glacet-Bernard,[1] Camille Jung,[2] Mathilde Goudot,[1] Alexandra Miere,[1] and Eric H. Souied[1]

[1]Department of Ophtalmology, Centre Hospitalier Intercommunal de Créteil, Créteil, France
[2]Centre de Recherche Clinique, Centre Hospitalier Intercommunal de Créteil, Université Paris Est, Créteil, France

Correspondence: Florence Coscas, Centre Hospitalier Intercommunal de Créteil, 40 Avenue Verdun, Université Paris Est, 94010 Créteil, France;
coscas.f@gmail.com.

FC and AS contributed equally to the work presented here and should therefore be regarded as equivalent authors.

Submitted: December 5, 2015
Accepted: April 17, 2016

Citation: Coscas F, Sellam A, Glacet-Bernard A, et al. Normative data for vascular density in superficial and deep capillary plexuses of healthy adults assessed by optical coherence tomography angiography. *Invest Ophthalmol Vis Sci*. 2016;57:OCT211–OCT223. DOI:10.1167/iovs.15-18793

Purpose. To establish a normative database for vascular density (VD) and foveal avascular zone (FAZ) at the superficial (SCP) and deep capillary plexus (DCP) in healthy subjects with optical coherence tomography (OCT) angiography.

Methods. The study was a retrospective chart review of healthy patients who had undergone OCT angiography imaging. A 3- × 3-mm area, centered on the fovea, was scanned for all the study eyes. The automated segmentation allowed separate analysis of the SCP, the DCP, and a comprehensive C-scan including both vascular layers. On the obtained images, VD and FAZ measurements were computed. Interobserver reproducibility and intraobserver repeatability were also assessed.

Results. A total of 135 eyes of 70 subjects (51% male) were analyzed. The mean age was 48.3 ± 17.5. We divided patients into group 1, from 20 to 39 years of age; group 2, from 40 to 59 years; and group 3, age 60 years or older. At the level of the SCP, mean VD and mean FAZ ± SD were, respectively, 52.58 ± 3.22% and 0.28 ± 0.1 mm^2. At the level of the DCP, mean VD and mean FAZ were 57.87 ± 2.82% and 0.37 ± 0.12 mm^2, respectively. The mean VD was significantly higher ($P < 0.05$) in DCP compared with SCP in all Early Treatment Diabetic Retinopathy Study (ETDRS) sectors and in all age groups. Vascular density was higher in women than in men after 60 years ($P < 0.01$). After adjustment on the signal strength index (SSI), the mean VD remained directly correlated with the age range and sex. The mean FAZ area was lower in group 3 ($P < 0.05$). Interobserver reproducibility was 0.78 to 0.99 in SCP and 0.67 to 0.92 in DCP, and intraobserver repeatability was 0.64 to 0.93 in SCP and 0.63 to 0.87 in DCP.

Conclusions. Our study has provided, for the first time, age-related VD mapping data using OCT angiography in healthy subjects. The prototype software used in this study may help to improve the concept of VD grading with high inter- and intraexaminer repeatability and interexaminer reproducibility.

Keywords: optical coherence tomography angiography, OCT angiography, normative database, vascular density, foveal avascular zone, nonflow area, superficial capillary plexus, deep capillary plexus, normal subject, healthy, adult

The human retina has the highest metabolic demand of any tissue in the body.[1] Because of its highly specialized activity, the ability to regulate blood flow is an essential and complex feature of the mammalian retina especially in the outer segments of the photoreceptors.[1] The histologic findings have identified four different retinal capillary plexuses, and only three of them are considered in the macula area: the superficial, the deep, and the intermediate capillary plexuses.[2–4] Recently, Spaide et al.[5] suggested that the intermediate capillary plexus could be mixed with the deep plexus itself. Moreover, in the same study, Spaide et al. stated that "the ganglion cell layer is invested with one or more layers of capillaries, and these were termed the inner vascular plexus" (p 47), proposing that one could study and try to quantify two different macular capillary layers: one superficial (inner) and one deep (outer), including the intermediate.

The vessels in the nerve fiber layer and the ganglion cell layer form the inner (or superficial) capillary plexus (SCP), while the inner plexiform layer and the outer plexiform layer receive blood from the deep capillary plexus (DCP) located in the junction between them.[6] The radial peripapillary capillary plexus is located in the nerve fiber layer in a small rim surrounding the optic nerve head.[7]

Fluorescein angiography has been the gold standard for imaging the retinal vasculature since its introduction in the 1960s.[8] However, fluorescein angiography is unable to individually evaluate the blood flow or vascular density (VD) in all these different plexuses. Optical coherence tomography angiography (OCT-A), recently introduced, provides a novel method for noninvasively imaging the capillary network and the foveal avascular zone (FAZ).[9] Also, OCT-A can use the split-spectrum amplitude-decorrelation angiography algorithm to

Investigative Ophthalmology & Visual Science

Table 1. Age-Related Vascular Density Mapping Data Using Optical Coherence Tomography Angiography in Healthy Subjects in a Comprehensive C-Scan Taken Between 3 μm Below the Internal Limiting Membrane and 70 μm Below the Internal Plexiform Layer, According to the Signal Strength Index (SSI)

	Age Range, y			
	29–39, $n = 48$ Eyes	40–59, $n = 41$ Eyes	>59, $n = 46$ Eyes	*P*
Mean VD in both plexuses (± SD)	57.7 (±2.5)	55.2 (±5.1)	51.9 (±8.3)	0.0001
Mean SSI (±SD)	80.4 (±5.3)	78.3 (±5.4)	73.3 (±4.9)	0.0001

detect erythrocyte movement.[10,11] Optical coherence tomography A has previously been used to describe the retinal vasculature in both normal eyes and various retinal vascular pathologies such as macular telangiectasia type 2, retinal vein occlusion, and diabetes.[12–15]

The AngioVue (Optovue, Inc., Fremont, CA, USA) is one of the currently commercially available OCT-A machines that allows a four-section division of the retina–choroid complex: superficial capillary plexus (SCP), DCP, outer retinal layers, and choriocapillaris. A new software update recently released by the AngioVue system allows quantification of the VD around the macula. Vascular density was defined as the percentage of the sample area occupied by vessel lumens following binary reconstruction of images. In vivo quantification of VD and the FAZ area may be useful in detecting and monitoring the progression of retinal vascular diseases such as diabetic retinopathy, retinal vein occlusion, and radiation retinopathy.[16–18]

A detailed search of published literature did not reveal any studies concerning VD in healthy subjects. Therefore, we performed this study to quantify VD and measure the FAZ area at the level of the superficial and deep capillary plexuses in healthy adults using OCT-A (AngioVue). We also evaluated the repeatability and reproducibility of VD and FAZ area measurements.

Methods

This study was a retrospective review of the case records of healthy subjects who had undergone OCT-A at the Créteil University Hospital between September 2015 and October 2015. This study was approved by the Institutional Review Board of Créteil Intercommunal Hospital and was conducted in accordance with the tenets of the 1964 Declaration of Helsinki.

Informed consent was obtained from all the study subjects before any of the study procedures were carried out. Subjects who had a best-corrected visual acuity (BCVA) of 20/20 or better with no history or clinical evidence of retinal disease were included in the study. Exclusion criteria were any history or clinical evidence of retinal disease, glaucoma, presence of macular edema, diabetic retinopathy, previous ocular surgery or laser photocoagulation, refractive error of 6 diopters or more, and signs of any other chorioretinal disease. Eyes with poor-quality images on OCT-A (signal strength index [SSI] lower than 50) due to eye movements or media opacities were also excluded.[12] The quality of the scans was indicated by a color scale at the bottom of the scan; it had to be in the green range to be considered a good-quality scan.

Table 2. Adjustment on Signal Strength Index Using Regression Analysis

Mean VD, $n = 135$ Eyes	Regression Coefficient	*P*	95% Confidence Interval
SSI	0.0261771	0.793	−0.17, 0.22
Age	−0.1226966	<0.0001	−0.19, −0.05

All study subjects were dilated with 1% tropicamide and 2.5% phenylephrine eye drops before examination. The initial evaluation of the study subjects included BCVA testing, intraocular pressure measurement, slit-lamp biomicroscopy, and fundus evaluation. All subjects then underwent imaging using the split-spectrum amplitude-decorrelation angiography algorithm (SSADA) on the AngioVue OCT-A system version 2015.100.0.35 (Optovue RTVue XR 100 AVANTI; Optovue, Inc.) intended for retinal imaging (AngioRetina mode). A 3- × 3-mm area, centered on the fovea, was scanned for all the study subjects in both eyes. The device performed each acquisition at a speed of 100 kHz, 70,000 A-scans per second, using an 840-nm superluminescent diode with a bandwidth of 45 nm; 304 A-scans made up a B-scan while 304 horizontal and vertical lines separated by 9 μm each were sampled in the scanning area in order to form a three-dimensional (3D) data cube. Volumetric raster scans were obtained from two horizontal fast transverse scans and two vertical fast transverse scans (2.9 seconds each). The calculated amplitude-decorrelation signal from the consecutive B-scans allowed blood flow and therefore the capillary network to be clearly visualized. Image analysis was performed by automated retinal segmentation derived from the machine software. Motion correction was performed using registration of two orthogonally captured imaging volumes.[19]

The SCP was imaged starting with the inner limiting membrane (ILM) and selecting sufficient thickness to include the ganglion cell layer, between 3 μm below the ILM and 15 μm below the inner border of the inner plexiform layer (IPL).

The deep plexus consisted of the capillaries in the area between 15 μm below the IPL (inner border) and 70 μm below the IPL (inner border). The inner nuclear layer is ordinarily bracketed by a layer of capillaries on either side.[20]

Moreover, a comprehensive C-scan taken between 3 μm below the ILM and 70 μm below the IPL, therefore including all the retinal vascular layers, was also assessed.

In order to evaluate age-related data, the study subjects were divided into three age groups: group 1 ranged from 20 to 39 years of age, group 2 ranged from 40 to 59 years, and group 3 consisted of subjects who were 60 years or older.

Vascular Density

Vascular density was defined as the percentage of the sample area occupied by vessel lumens following binary reconstruction of images. The percentage of vessels was defined in the sectors (superior, temporal, inferior, and nasal) based on the Early Treatment Diabetic Retinopathy Study (ETDRS) chart where the fovea center was automatically determined from the relevant OCT data. The inner and outer rings with a diameter of 1 and 2.5 mm around the fovea were respectively considered for evaluation.

We used the flow density map software AngioAnalytics (version 2015.100.0.35), the world's first OCT-A automatic quantification tool that measures flow area, nonflow area, and flow area density. AngioAnalytics evaluates and then reports the relative density of flow as a percentage of the total

Table 3. Normative Data of Vascular Density in Superficial Capillary Plexus; Percentage of Vessels Was Defined in Sectors Based on the ETDRS Chart (Superior, Temporal, Inferior, and Nasal) Where the Fovea Center Was Automatically Determined from the Structure OCT Data, and the Inner and Outer Diameters of the Parafoveal Region Were 1 and 2.5 mm

	Whole En Face, %	Fovea, %	Parafovea, %	T, %	S, %	N, %	I, %	FAZ, mm²
Group 1, 20–39 y, $n = 48$ eyes	53.91 ± 2.09	31.31 ± 4.81	55.70 ± 2.25	54.23 ± 2.86	57.21 ± 2.48	54.51 ± 2.37	56.71 ± 2.33	0.27 ± 0.10
Group 2, 40–59 y, $n = 41$ eyes	53.56 ± 2.23	30.31 ± 4.30	55.59 ± 2.22	54.53 ± 2.33	56.58 ± 2.52	54.57 ± 2.94	56.71 ± 2.44	0.30 ± 0.09
Group 3, >60 y, $n = 46$ eyes	50.35 ± 3.77†	32.81 ± 5.19*	51.79 ± 4.09†	50.88 ± 4.46†	51.66 ± 6.02†	50.98 ± 4.39†	53.39 ± 4.97†	0.23 ± 0.08*
Total, $n = 135$ eyes	52.58 ± 3.22	31.52 ± 4.87	54.33 ± 3.50	53.18 ± 3.73	55.13 ± 4.75	53.34 ± 3.72	55.58 ± 3.80	0.28 ± 0.10

T, temporal; S, superior; N, nasal; I, inferior.
* $P < 0.05$.
† $P < 0.01$.

evaluated area. With AngioAnalytics software, VD is calculated by first extracting a binary image of the vessels from the grayscale OCT-A en face image, and then computing the percentage of pixels of vessels in the defined sectors or in the entire en face image based on the binary image.

In order to exclude that the quantitative assessment might be influenced by the image quality, a regression analysis was performed in order to examine a potential association between age, SSI, and mean VD measures. To evaluate the association between age on SSI and mean vessel density measures, univariate and multivariate analyses were performed using linear regression method. These analyses took into account the three age ranges (20–39 years; 40–59 years; and >59 years).

Measurement of FAZ Area

Automated measurement of the FAZ area was obtained using the new nonflow area measurement option. An avascular area defined by automatic border detection was quantified. The reference section or determination of the superficial plexus was defined within a distance of 60 μm starting from the ILM. Two graders (FC and AS) performed measurements of the FAZ area using the acquired images. Optical coherence tomography A images at the level of the superficial and deep capillary plexuses were measured by clicking on the center of the FAZ.

Reproducibility and Repeatability

Reproducibility and repeatability are indicators of the applicability of any instrument as a diagnostic tool in clinical practice. They refer to the degree of agreement between independent measurements that are obtained with the same method or instrument on identical test material under different conditions (i.e., different operators) or under the same conditions (i.e., same operator performing consecutive measurements). The coefficient of variation was used to evaluate between-day reproducibility and within-day repeatability. The study subjects underwent two imaging sessions within a single visit. This session was repeated once during the study period by a single examiner (FC). The measurements of VD and FAZ area were performed by two independent experienced examiners (FC, AS) (twice, 1 minute apart: T0 and T1) and repeated once by one of the examiners 30 days later (T2). Thus, three measurements were obtained for each patient.

Statistical Analysis

The nonparametric Mann-Whitney and Kruskal-Wallis tests were used to compare the statistical distribution of the SSI with the measures of the mean inner retinal VD considering both sex and age range.

Qualitative variables were described in percentages, and quantitative variables were described by their mean and standard deviation (SD). Depending on the distribution, comparisons of means or medians of independent variables were performed using Student's *t*-test, Mann-Whitney test, or Kruskal-Wallis test in the case of three groups. The paired *t*-test was used to compare paired data. Bland-Altman plots, intraclass correlations (with 95% confidence intervals [CIs]), and measures of the coefficient of repeatability (CR) (1.96 times the SD of the differences between the two measurements) were used to evaluate the inter- and intraexaminer reproducibility of the measurements. The coefficients of variation (SD/mean) were calculated for each variable measured by the first

Table 4. Normative Data of Vascular Density in Deep Capillary Plexus; Percentage of Vessels Was Defined in Sectors Based on the ETDRS Chart (Superior, Temporal, Inferior, and Nasal) Where the Fovea Center Was Automatically Determined From the Structure OCT Data, and the Inner and Outer Diameters of the Parafoveal Region Were 1 and 2.5 mm

	Whole En Face, %	Fovea, %	Parafovea, %	T, %	S, %	N, %	I, %	FAZ, mm²
Group 1, 20–39 y, $n = 48$ eyes	59.36 ± 1.74	30.09 ± 5.99	61.90 ± 1.77	60.59 ± 2.29	63.35 ± 2.22	60.80 ± 2.16	62.86 ± 1.92	0.37 ± 0.11
Group 2, 40–59 y, $n = 41$ eyes	58.06 ± 2.21	30.01 ± 6.63	60.65 ± 1.95	59.78 ± 1.95	61.46 ± 2.11	59.34 ± 3.00	61.71 ± 2.65	0.39 ± 0.13
Group 3, >60 y, $n = 46$ eyes	56.15 ± 3.28*	32.05 ± 6.19	58.11 ± 3.81*	56.49 ± 4.67*	58.81 ± 5.48*	56.88 ± 4.00*	60.24 ± 3.91*	0.37 ± 0.10
Total, $n = 135$ eyes	57.87 ± 2.82	30.73 ± 6.28	60.23 ± 3.11	58.95 ± 3.68	61.23 ± 4.10	59.02 ± 3.53	61.62 ± 3.12	0.37 ± 0.12

* $P < 0.01$.

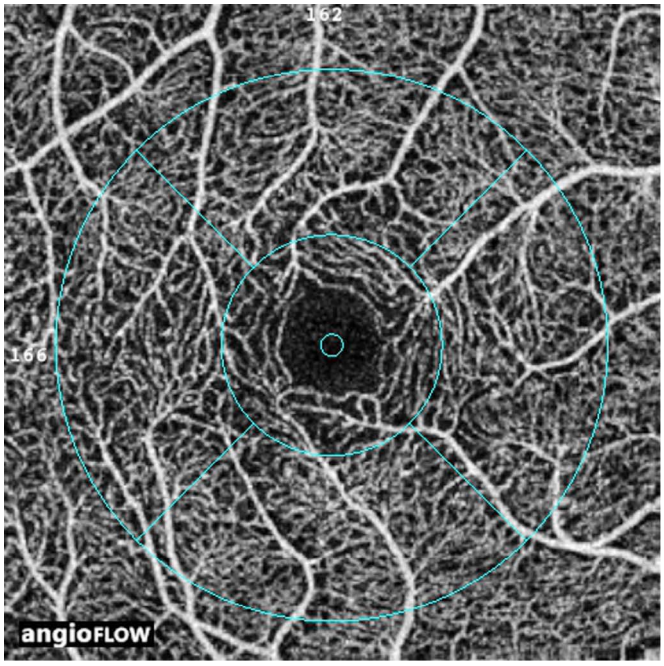

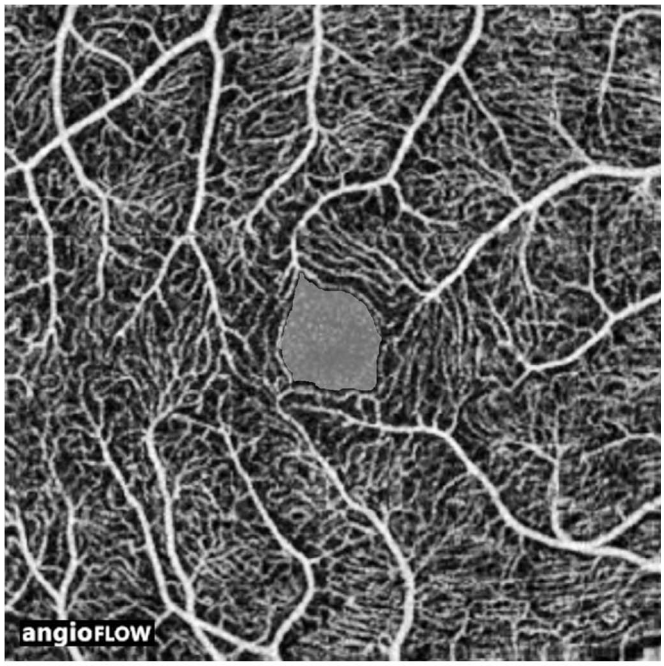

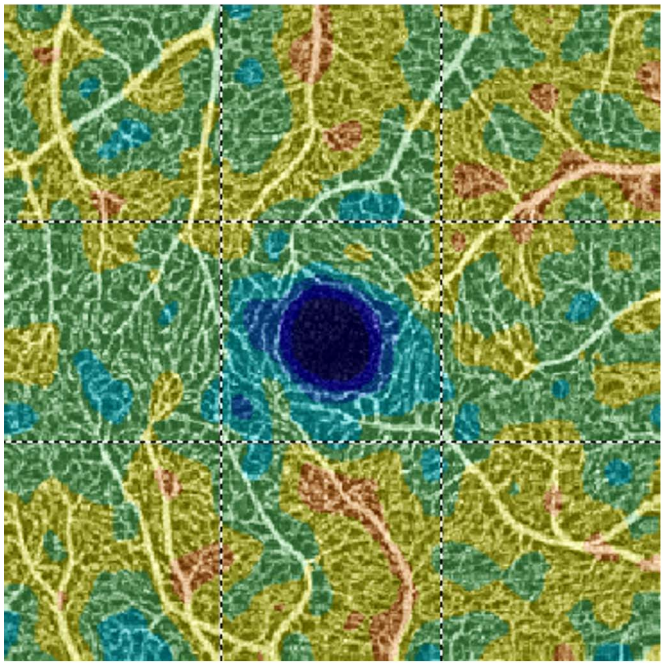

OCT Thickness ILM-RPE & Flow Density

Section	Thickness (µm)	Density (%)
Whole en face	N/A	54.20
Fovea	285	33.65
ParaFovea	332	56.01
- Tempo	321	52.95
- Superior	329	55.83
- Nasal	341	56.46
- Inferior	336	58.83

Figure 1. Optical coherence tomography angiography, healthy subject, at the superficial capillary plexus (age: 26, group 1). (**A**) ETDRS grid on 10° central macula with foveal ring (1 mm), four quadrants (superior, inferior, temporal, and nasal 2.5 mm). (**B**) The foveal avascular zone is the central nonflux zone (translucent white color), normal in this case (0.201 mm^2) in our study. (**C**) Normal virtual colored macular vascular density is normal (54.20%) in whole en face. (*Dark blue* to *light blue* areas indicate areas of no flow to low flow density, respectively. *Green* indicates an area of medium flow density; *yellow* indicates an area of medium-high flow density; *red* indicates an area of high flow density.) These automatic measures of central nonflux area are unchangeable manually.

examiner to compare the dispersion of the measures of VD and FAZ area. A P value < 0.05 was considered statistically significant. All statistical analyses were performed with STATA version 13.0 (Stata Corp LP, College Station, TX, USA).

Results

A total of 135 eyes of 70 Caucasian subjects (69 eyes of males, 51%) were included in this study, of which 48 eyes were in group 1 (20–39 years old), 41 in group 2 (40–59 years old), and 46 in group 3 (60 years and older). All study measurements provided high-quality scans. The mean age of the study subjects was 48.3 years (SD 17.5 years; range, 20–79 years).

There was a statistically significant difference ($P = 0.0001$) between the mean VD of a comprehensive C-scan including both vascular plexuses and different age ranges (Table 1).

In univariate analysis, age ranges were associated with SSI ($P < 0.0001$) and mean VD ($P < 0.0001$). In multivariate analysis, age was significantly associated with SSI whereas age

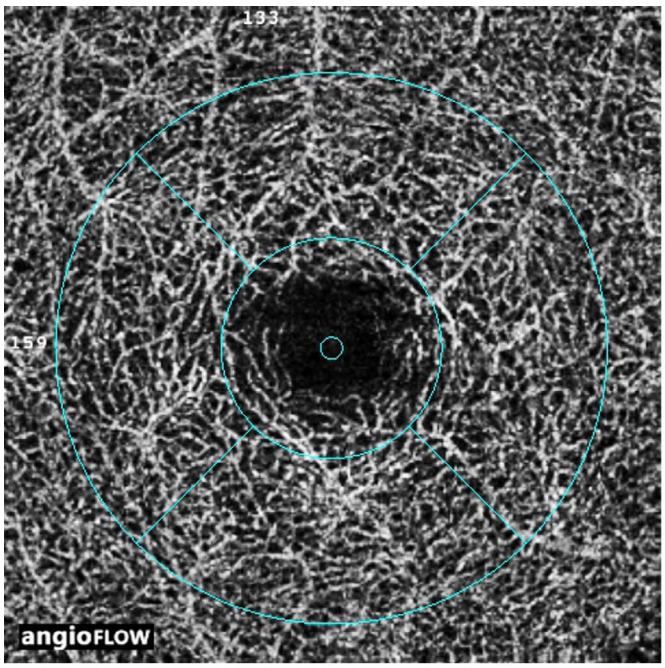

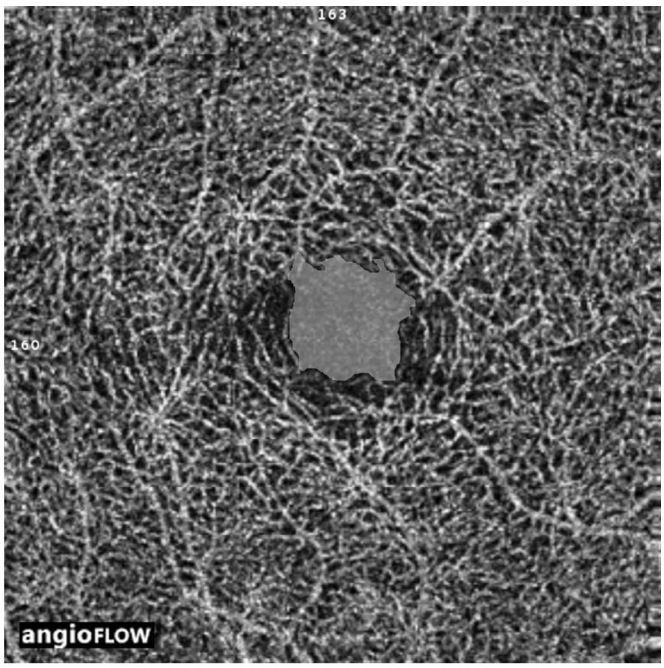

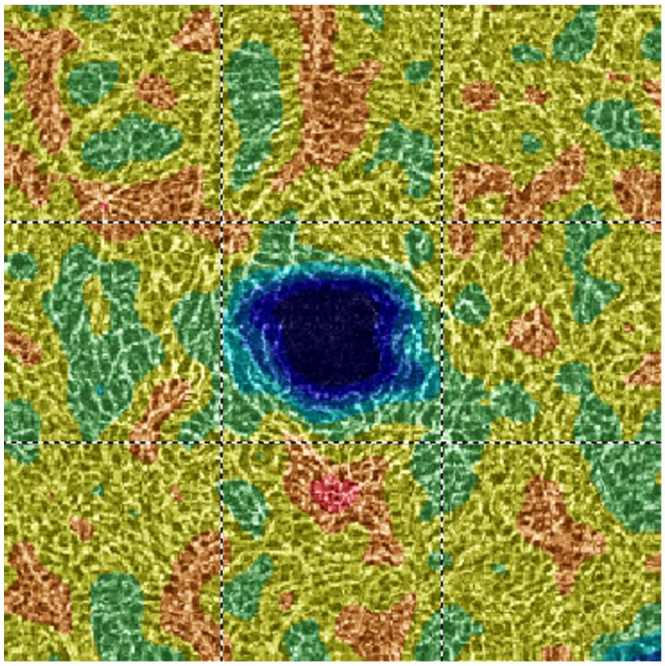

OCT Thickness ILM-RPE & Flow Density

Section	Thickness (µm)	Density (%)
Whole en face	N/A	58.54
Fovea	285	30.85
ParaFovea	332	61.00
- Tempo	321	58.90
- Superior	329	61.42
- Nasal	341	60.92
- Inferior	336	62.80

Figure 2. Optical coherence tomography angiography, same healthy subject as in Figure 1, at the deep capillary plexus. (**A**) ETDRS grid on 10° central macula. (**B**) The foveal avascular zone is the central nonflux zone (translucent white color), larger than at the superficial level (0.396 mm^2). (**C**) Normal virtual colored macular vascular density (58.54% whole en face).

range 40 to 59 and >59 were associated with mean VD measures. After adjustment on SSI using regression analysis, VD was still associated with age (Tables 1, 2).

Overall, at the level of the SCP, the mean VD and mean FAZ area were respectively 52.58 ± 3.22% and 0.28 ± 0.1 mm^2 in the whole en face image. At the level of the DCP, mean VD and mean FAZ area were respectively 57.87 ± 2.82% and 0.37 ± 0.12 mm^2 in the whole en face image.

The mean VD and FAZ area, according to the ETDRS sectors and the three age groups, in both the superficial and deep capillary plexuses are shown in Tables 3 and 4. Several healthy subjects with different sizes of FAZ and VD are depicted in Figures 1 to 6. The mean VD results revealed that it was significantly higher ($P < 0.05$) in DCP compared with SCP in all ETDRS sectors and in all age groups. Also, the superior and inferior sector mean VDs were higher ($P < 0.001$) than those in the temporal and nasal sectors in both plexuses and in all age groups.

There was no statistically significant difference between groups 1 and 2 for the mean VD in the foveal ring (1 mm around the fovea) and in every quadrant (2.5 mm around the fovea). However, the mean VD in group 3 was lower ($P < 0.01$) compared with the other groups in both plexuses and in every ring and sector. The mean VD was higher ($P < 0.05$) in women in every quadrant in both plexuses.

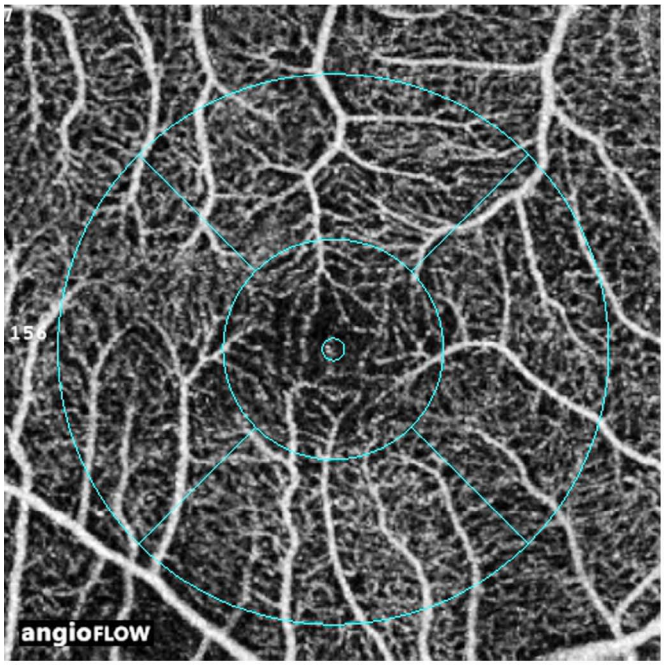

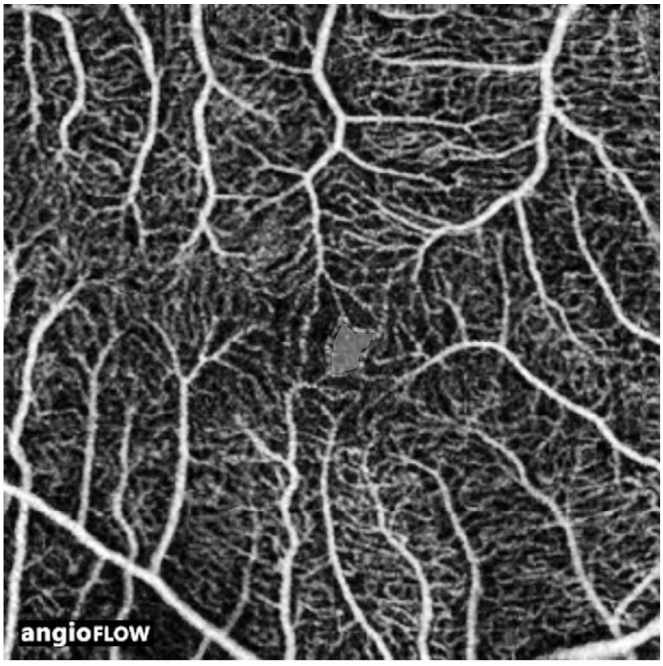

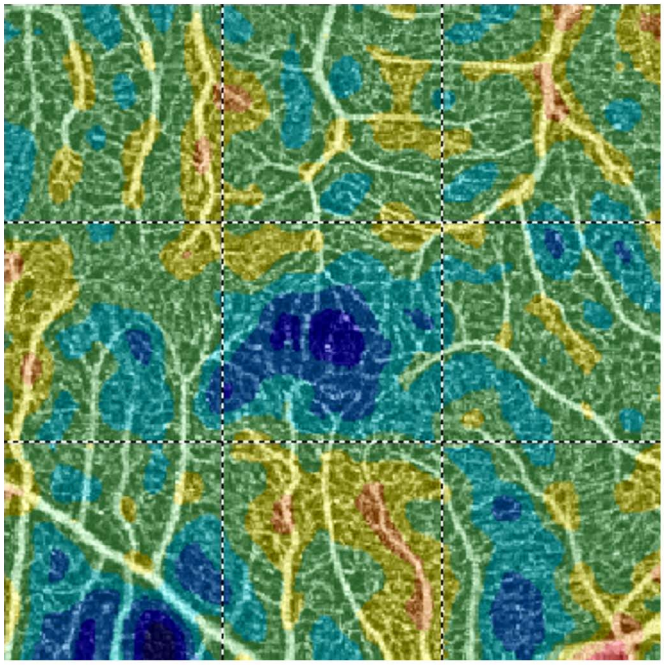

OCT Thickness ILM-RPE & Flow Density

Section	Thickness (µm)	Density (%)
Whole en face	N/A	49.20
Fovea	293	35.63
ParaFovea	328	50.94
- Tempo	320	48.60
- Superior	329	53.04
- Nasal	332	47.99
- Inferior	330	54.14

Figure 3. Optical coherence tomography angiography, another healthy subject with a small foveal avascular zone, at the superficial capillary plexus (age: 54, group 2). (**A**) ETDRS grid on 10° central macula. (**B**) The foveal avascular zone (translucent white color) is very small in this case (0.06 mm^2). (**C**) Normal virtual colored macular vascular density (49.20% whole en face).

The mean FAZ area was smaller ($P < 0.05$) in group 3 compared with groups 1 and 2 at the level of the SCP. There was no statistically significant difference for the mean FAZ in the three groups at the level of the DCP. There was no statistically significant difference ($P > 0.05$) between the fellow eyes of the study patients for both VD and FAZ.

The intraclass correlation coefficient (ICC) is the ratio of the intersubject component of the variance to the total variance. The indicators of repeatability (CR), coefficient of variation (CV), and ICC of the VD and FAZ area are reported in Tables 5 (SCP) and 6 (DCP) as calculated from the means of the Bland-Altman plots. Inter- and intraobserver ICCs for the VD in all rings and quadrants are shown in Tables 5 (SCP) and 6 (DCP) and Figure 7 (graph of the dispersion table). Tables 5 and 6 show interobserver intrasession ICC values ranging from 0.70 to 0.99 in the SCP and from 0.67 to 0.92 in the DCP; intraobserver intersession reproducibility ICC values ranged from 0.64 to 0.93 in the SCP and from 0.63 to 0.87 in the DCP. Interobserver ICC was 0.96 (95% CI 0.94–0.98), and intraobserver ICC was 0.85 (95% CI 0.78–0.93) for FAZ at the SCP and DCP.

Discussion

Spectral-domain OCT (SD-OCT) has recently emerged as a useful imaging technique that provides reliable, highly

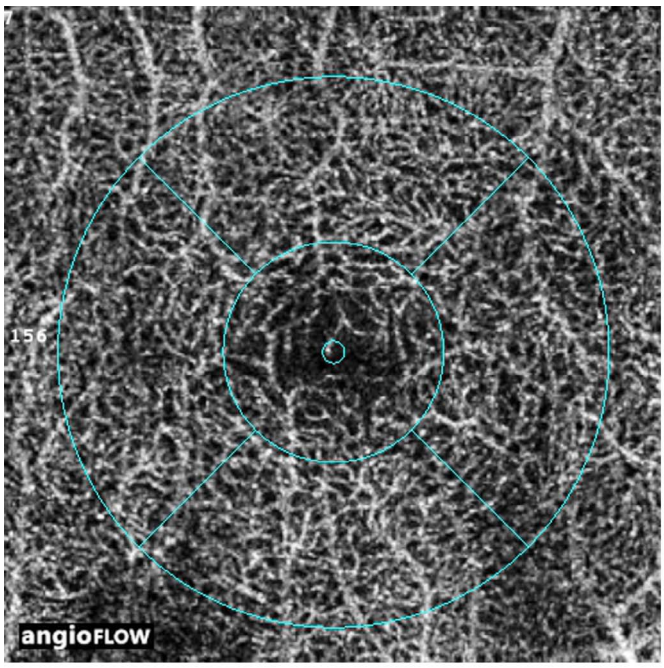

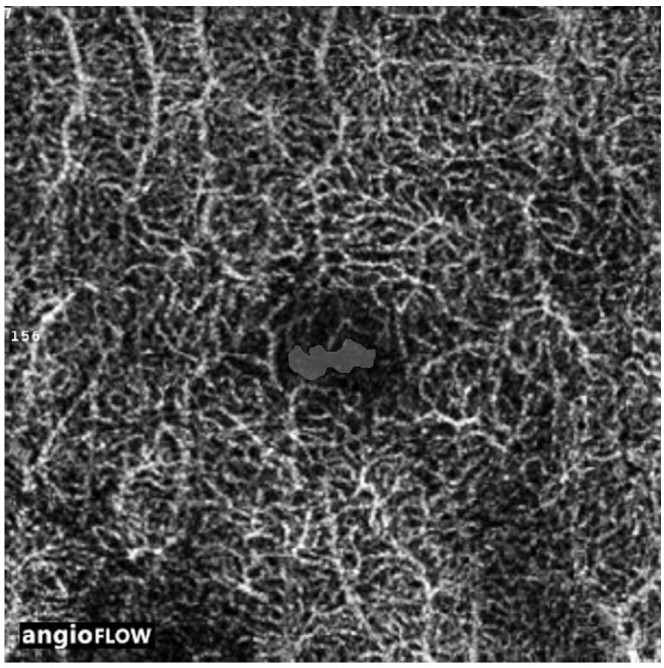

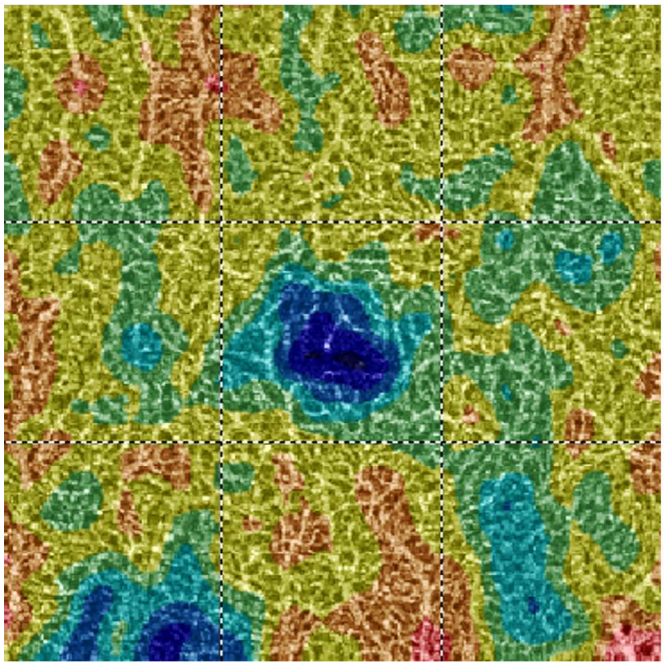

OCT Thickness ILM-RPE & Flow Density

Section	Thickness (μm)	Density (%)
Whole en face	N/A	57.81
Fovea	293	40.58
ParaFovea	328	59.08
- Tempo	320	58.21
- Superior	329	60.98
- Nasal	332	54.74
- Inferior	330	62.38

FIGURE 4. Optical coherence tomography angiography, same healthy subject as in Figure 3, at the deep capillary plexus. (**A**) ETDRS grid on 10° central macula. (**B**) The foveal avascular zone is the central nonflux zone (translucent white color) and is larger than at the superficial level (0.087 mm^2). (**C**) Normal virtual colored macular vascular density (57.81%).

reproducible, and high-resolution cross-sectional images and valuable anatomic information for the macula. The quantification of macular thickness by SD-OCT is now a reproducible and noninvasive technique[21] that enables clinicians to monitor the efficacy of treatment for macular pathologies such as diabetic or venous macular edema. Previous studies with SD-OCT[21,22] and swept-source OCT have provided sex- and age-related central macular thickness data in normal subjects.

Optical coherence tomography A, a noninvasive imaging technique that does not require any dyes, enables the imaging of blood vessels based on flow characteristics and provides improved information on retinal and choriocapillaris microvasculature compared with conventional fluorescein angiography.[5,23] Optical coherence tomography A has already proved successful at qualitatively imaging the microvascular changes in diabetic retinopathy, retinal venous or arterial occlusion, choroidal neovascularization, and glaucoma.[13,14,24–27] A novel software program recently released by the AngioVue system enables the quantitative evaluation of such microvascular changes.

Our quantitative results demonstrate excellent interobserver intrasession ICCs (ranging from 0.7 to 0.99 in the SCP and from 0.67 to 0.92 in the DCP) and substantial intraobserver intersession reproducibility (from 0.64 to 0.93 in the SCP and from 0.63 to 0.87 in the DCP) in both plexuses. The estimate of the effect of the observer, which indicates the bias between

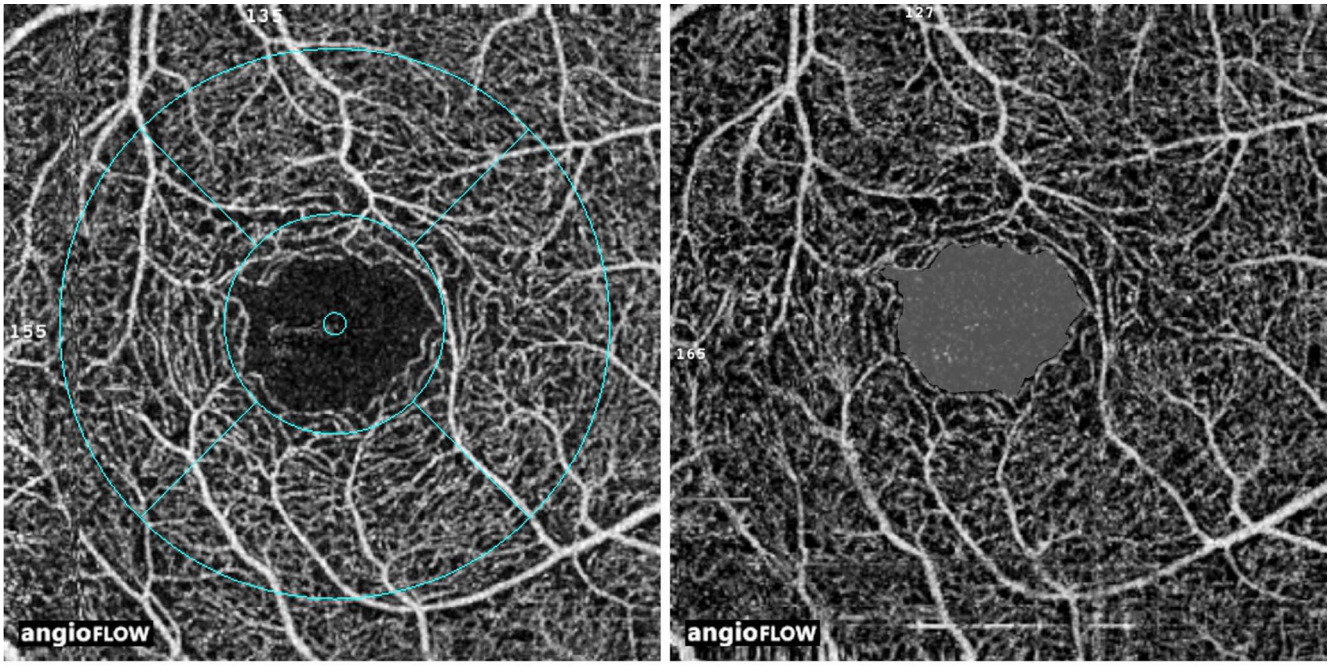

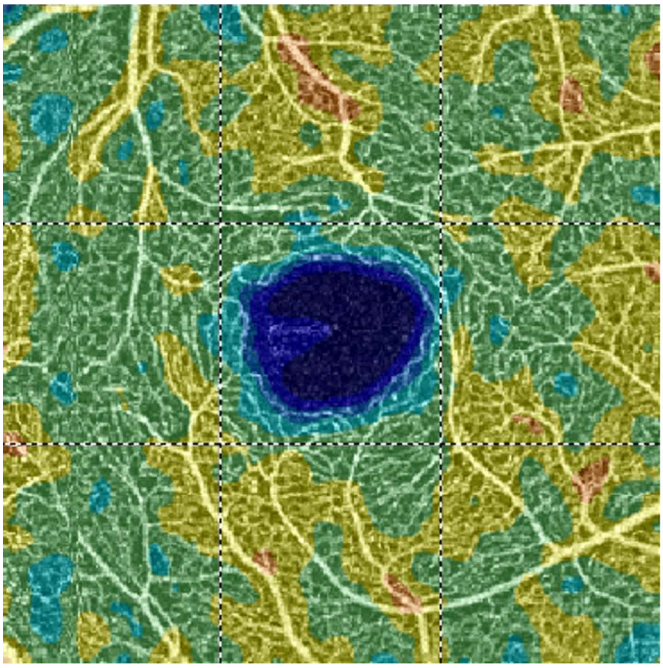

OCT Thickness ILM-RPE & Flow Density

Section	Thickness (μm)	Density (%)
Whole en face	N/A	51.83
Fovea	235	22.07
ParaFovea	323	54.58
- Tempo	314	51.94
- Superior	333	55.02
- Nasal	319	55.24
- Inferior	325	56.12

FIGURE 5. Optical coherence tomography angiography, healthy subject with large foveal avascular zone, at the superficial capillary plexus (age: 31, group 2). (**A**) ETDRS grid on 10° central macula. (**B**) The foveal avascular zone (translucent white color) is very large (0.489 mm^2). (**C**) Normal virtual colored macular vascular density (51.83%).

observers, was not statistically significant for any of the tested parameters. The ICCs of VD measurements were not statistically significantly different between the two sessions or between the two examiners in both the deep and superficial capillary plexuses. The coefficient of reproducibility showed good reliability and homogeneity of all the measurements, while the CV showed statistically low dispersion of the measurements in both plexuses for all the studied parameters.

Vascular Density

This study has provided, for the first time, VD mapping data using OCT-A in three groups of healthy adults ranging from 20 to 79 years of age. To the best of our knowledge, no such age-related OCT-A data have been available concerning macular VD in the 10° central and nonflow central areas.

We observed that the variability in VD increases with age. Vascular density was also higher ($P < 0.01$) in the DCP compared with the SCP. This is probably because the DCP is composed of the homogenous capillary vortex[28] and the ramifications converging radially toward an epicenter, whereas the SCP is formed only by transverse capillaries. Another possibility is that the segmentation of the DCP assessed by the AngioVue also contains some capillaries from the superficial layer and artificially elevates the VD of the DCP. The only flow index and VD studies already

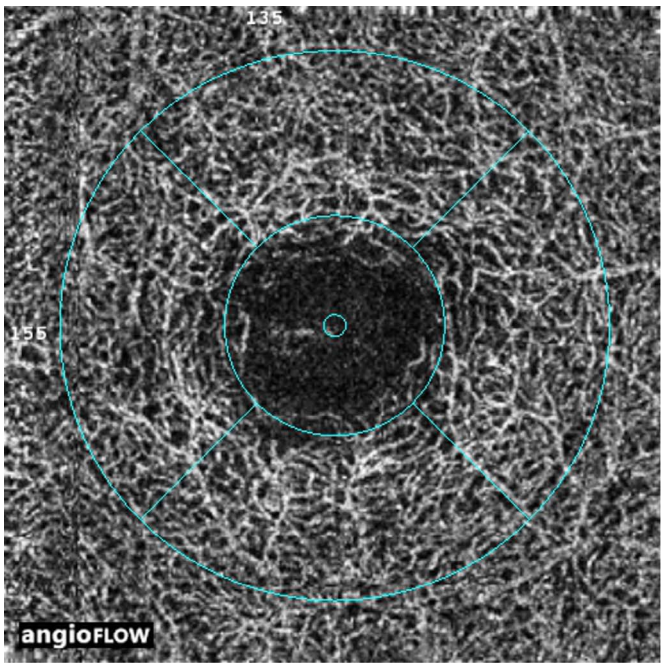

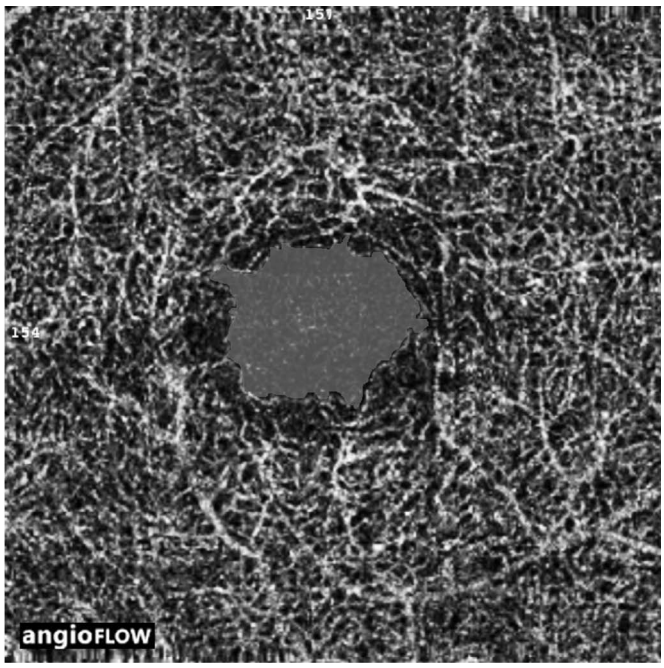

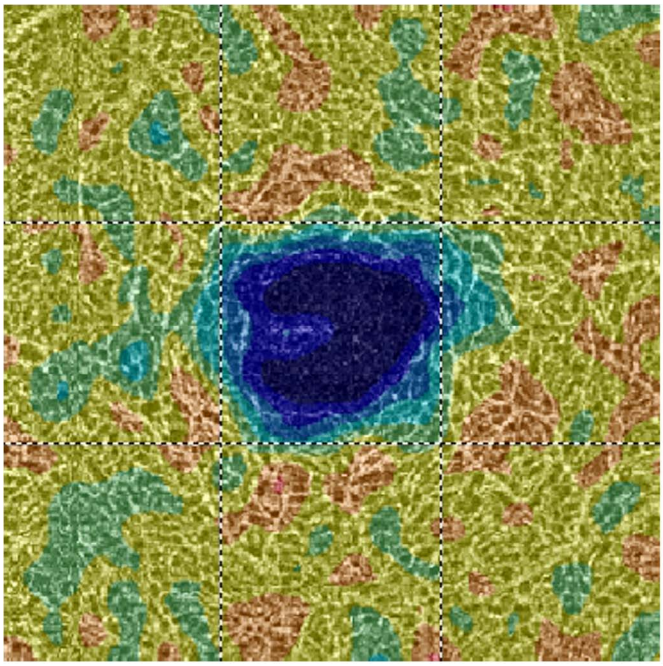

OCT Thickness ILM-RPE & Flow Density

Section	Thickness (µm)	Density (%)
Whole en face	N/A	56.96
Fovea	235	16.14
ParaFovea	323	60.06
- Tempo	314	57.77
- Superior	333	61.68
- Nasal	319	59.84
- Inferior	325	60.97

FIGURE 6. Optical coherence tomography angiography, same healthy subject as in Figure 5, at the deep capillary plexus. (**A**) ETDRS grid on 10° central macula. (**B**) The foveal avascular zone (translucent white color) is larger than at the superficial level (0.76 mm^2). (**C**) Normal virtual colored macular vascular density (56.96%).

reported used skeletonized images of OCT-A (ImageJ protocol) in open-angle glaucoma or diabetic patients; these studies compared patient-related data with a small sample of age-matched healthy controls.[16,25]

We have computed the VD for the whole inner retina in addition of those of the two single plexuses, showing a significant decrease in terms of VD according to the age range.

No statistically significant correlation was noticed between the SSI and the vessel's density value considering the SCP, the DCP, or the full retinal vascular thickness. After adjustment on SSI using regression analysis, VD was still associated with age.

Foveal Avascular Zone

The FAZ is the macular capillary-free zone that is used as an anatomic reference mark for locating the retinal point of fixation and is surrounded by interconnected retinal capillary plexuses. Its size as measured by fluorescein angiography reflects the status of the microcapillary circulation in the foveal area.[29–32] Also, the FAZ area has a strong positive correlation with the degree of capillary nonperfusion in diabetic retinopathies.[33,34] We observed that the FAZ area was larger ($P < 0.001$) in the DCP than in the SCP. There were no statistically significant differences between groups 1 and 2 for any of the parameters studied in both plexuses.

Table 5. Inter- and Intraobserver Repeatability of Measurements of Vessel Density With OCT Angiography in the Superficial Capillary Plexus

	Interobserver Reproducibility of Measurement			Intraobserver Reproducibility of Measurement	
	ICC (95% CI)	CV, %	CR	ICC (95% CI)	CR
Whole en face	0.79 (0.68–0.89)	6	4.03	0.73 (0.58–0.88)	4.7
Fovea	0.89 (0.84–0.95)	15	4.23	0.93 (0.89–0.97)	4.28
Parafovea	0.82 (0.73–0.91)	6	6.58	0.78 (0.65–0.91)	3.32
Temporal	0.82 (0.73–0.91)	7	4.2	0.83 (0.73–0.93)	4.99
Superior	0.84 (0.77–0.92)	8	4.89	0.79 (0.66–0.91)	3.32
Nasal	0.99 (0.995–0.998)	7	5.02	0.64 (0.45–0.83)	4.52
Inferior	0.78 (0.68–0.89)	7	4.8	0.68 (0.50–0.86)	4
FAZ	0.96 (0.94–0.98)	36	0.05	0.85 (0.78–0.93)	0.09

ICC, intraclass correlation coefficient ratio of the intersubject component of the variance to the total variance. The higher the ratio, the better the repeatability. All results indicate ICC value. Strength of agreement beyond chance is fair between 0 and 0.25, moderate between 0.26 and 0.50, substantial between 0.51 and 0.75, and almost perfect between 0.76 and 1.00.

Evaluation of the reproducibility and repeatability of FAZ area measurements in young patients using OCT-A has been previously published.[35] Other studies concerned FAZ measurements in diabetic patients.[14,16,26,36] These studies have described the FAZ size and shape in healthy populations, but they used various imaging modalities and software, focused only on the FAZ at the level of the SCP, and did not distinguish between the different age groups. More recently, Samara et al.[37] showed that the manually selected deep FAZ area was significantly larger than the superficial FAZ area; this is consistent with our study (Table 7).

Previous studies of FAZ mainly used ImageJ software (an external publicly available image processing program developed by Wayne from the Ocular Oncology Service, Wills Eye Hospital, Thomas Jefferson University, Philadelphia, PA, USA, supported by Eye Tumor Research Foundation, Philadelphia).[12,16,36,37] ImageJ with manual tracks creates binary images for better contrast and the identification of erroneous autosegmentation. In these studies, mean FAZ area varied from 0.25 to 0.34 mm^2 except with swept-source OCT-A,[38] which, using a full-spectrum algorithm, gave measurements that were slightly larger but closer to fluorescein angiography measurements (Table 7).

In a study of 60 healthy eyes using the same software as ours (AngioAnalytics), the FAZ area was 0.251 ± 0.096 mm^2 with high repeatability and reproducibility. However, the mean age of the study population was 28.9 ± 7.6 years, and there was no analysis of its variation in the different age groups.[35] In our Caucasian population, the superficial FAZ area was 0.28 ± 0.10 for a mean age of 48.3 ± 17.5 years. This small difference may be explained by our study population since we did not exclude patients with small or large FAZ areas (range, 0.086–0.554; Figs. 1, 2). The FAZ was considered very small (<0.15 mm^2) in 9 eyes (Figs. 3, 4) and very large (>0.5 mm^2) in 10 eyes. Eyes with a very small FAZ had increased VD (Figs. 5–7).

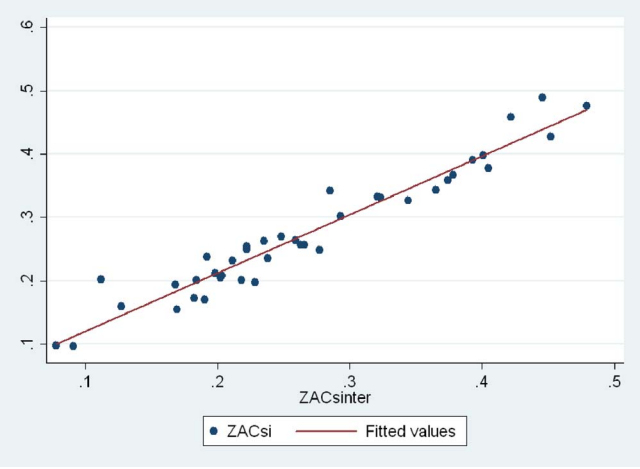

Figure 7. Scatter plot of the foveal avascular zone measurement by two observers showing excellent reproducibility. Dispersion of the measurements is very important.

We observed that the superficial FAZ area was significantly smaller in the older age group; this is probably due to a decrease in the perifoveal VD in the elderly. These results confirm the existence of an age-related reduction in the FAZ area that may be explained by atrophic and occlusive changes in the macular capillaries.[39] It may be that these capillary plexuses have unique relationships only at the fovea (i.e., they intersect at the FAZ) even where the DCP layers otherwise are laminar and intersect only with vertical connecting vessels. As such, the segmentation may break down at the FAZ. This explains why the FAZ at the DCP may look larger—because these vessels are actually moving into the IPL/ganglion cell layer as all of these anatomic layers narrow at the fovea.

In our study, we obtained high inter- and intraobserver repeatability for the SCP and DCP for the FAZ area measurements. The central foveal avascular area appeared to be significantly greater in the DCP (0.37 ± 0.12) than in the SCP (0.28 ± 0.10) as in a previous study. We also observed this difference between the two plexuses in all our age groups. It is possible that the FAZ border may be accurately outlined, considering the perifoveal arcade, only in the SCP.

Vascular density was significantly higher in both the superior and inferior sectors of the central area compared with the nasal and temporal sectors. These results were not expected considering the work of Hayreh[40] on the watershed zones: Blood flow to the temporal retina was approximately three times larger than that to the nasal retina, with no difference between the superior and inferior retina. Our study showed no significant ($P > 0.05$) difference between the fellow eyes of our study patients for any of the study parameters, as expected. Vascular density was higher ($P < 0.01$) in women than in men after 60 years of age, probably due to late vascular aging in females.

The high reproducibility and repeatability of the VD measurements in all macular sectors including the nonflow central area enabled us to establish an age-related baseline database in healthy subjects. Reproducibility and repeatability were also high in older subjects, probably due to the SSADA algorithm included in the AngioVue software. However, the automatic segmentation in the SSADA algorithm does not accurately distinguish between the superficial and deep capillary plexuses. Also, the projection artifact, as described

Table 6. Inter- and Intraobserver Repeatability of Measurements of Vessel Density With OCT Angiography in the Deep Capillary Plexus

	Interobserver Reproducibility of Measurement			Intraobserver Reproducibility of Measurement	
	ICC (95% CI)	CV%	CR	ICC (95% CI)	CR
Whole en face	0.74 (0.62–0.87)	5	3.84	0.51 (0.27–0.76)	4.7
Fovea	0.92 (0.89–0.96)	20	4.37	0.87 (0.80–0.95)	4.28
Parafovea	0.81 (0.71–0.90)	5	3.64	0.74 (0.60–0.89)	3.32
Temporal	0.77 (0.66–0.89)	6	4.71	0.68 (0.51–0.86)	4.99
Superior	0.79 (0.69–0.90)	6	4.9	0.81 (0.70–0.93)	3.32
Nasal	0.72 (0.59–0.86)	6	5.02	0.63 (0.43–0.83)	4.52
Inferior	0.67 (0.52–0.83)	5	4.56	0.65 (0.46–0.84)	4
FAZ	0.96 (0.94–0.98)	38	0.05	0.86 (0.77–0.94)	0.09

ICC, intraclass correlation coefficient ratio of the intersubject component of the variance to the total variance. The higher the ratio, the better the repeatability. All results indicate ICC value. Strength of agreement beyond chance is fair between 0 and 0.25, moderate between 0.26 and 0.50, substantial between 0.51 and 0.75, and almost perfect between 0.76 and 1.00.

by Spaide et al.,[41] and other identified artifacts[42] could induce some difficulties during interpretation of the obtained images. In our study of healthy subjects, we always obtained sufficient signal-to-noise ratio in both the SCP and DCP plexuses and experienced no loss of long fixation due to the blue fixation light. Regarding projection artifacts and those related to segmentation of individual vessel layers, it is necessary to bear these in mind as well as the effects of segmentation errors on the interconnected anastomoses between the SCP and DCP.[28] We are aware of the effect of flow projection on quantitative data, but, since the same decorrelation algorithm is used for the follow-up scans, it will not affect the results of any comparative study.

Limitations of our study are related to the thickness of segmentation and the difficulties in discriminating the nonflow area of the FAZ due to the thresholding method that can underestimate VD in regions of higher VD.[13] We measured foveal VD using the AngioAnalytics software; this was 31.52 ± 4.87% at the SCP and 30.73 ± 6.28% at the DCP. However, this 1-mm ring around the fovea is a capillary-free zone, and our measurement may be an artifact from the software overestimating the VD in this area. Therefore, we did not include this measurement in our study analyses.

The flow projection artifact could be a relative issue and influence the quantitative analysis; however the current segmentation has been used in numerous published studies that provided both a qualitative[11] and quantitative[43] assessment of the different vascular layers.

In conclusion, our study has provided, for the first time, age-related VD mapping data using OCT-A in healthy subjects. The

Table 7. Comparison of Superficial FAZ Area Using Different Imaging Modalities in Healthy Eyes According to Age

Authors	Technique/Algorithms	Diseased Subjects	Healthy Subjects' Eyes (Subjects)	Healthy Mean Age	Healthy Mean FAZ Area
Bresnick et al.,[33] 1984	Argentic FA	36	20	44 (24–52)	0.35 mm²
Arend et al.,[34] 1991	Scanning laser ophthalmoscope FA	48	21	26 ± 4	0.231 ± 0.06 mm²
Tam et al.,[30] 2010	Adaptive optics scanning laser ophthalmoscope	None	10	27 ± 6.4	0.323 ± 0.107 mm²
John et al.,[29] 2011	Contrast-adjusted scanning laser ophthalmoscope FA	None	31	29.7 (20–40)	0.275 ± 0.074 mm²
Kim et al.,[31] 2012	Phase-variance optical coherence tomography	8	2	54 (29–66)	<0.2 mm²
Chui et al.,[32] 2014	Adaptive optics scanning laser ophthalmoscope microangiography	No	32	Nd (22–61)	0.32 ± 0.16 mm²
De Carlo et al.,[17] 2015	OCT angiography ImageJ*	39	28 (22)	54 ± 11.61	0.348 (0.1085–0.671) mm²
Freiberg et al.,[26] 2015	OCT angiography ImageJ*	37	25 (22)	60.41 ± 20.35	0.661 ± 0.171, max vertical diameter
Kuehlewein et al.,[38] 2015	Swept-source OCT microangiography	None	19 (13)	31 ± 5 (26–41)	0.304 ± 0.132 mm²
Carpineto et al., [35] 2016	OCT angiography AngioAnalytics†	None	60 (60)	28.9 ± 7.6	0.251 ± 0.096 mm²
Samara et al.,[37] 2015	OCT angiography ImageJ*	None	67 (70)	42 (41, 12–76)	0.266 ± 0.097 mm²
Takase et al.,[36] 2015	OCT angiography ImageJ*	24	19 (Nd)	62.8 ± 11.3 (38–81)	0.25 ± 0.06 mm²
Coscas et al. (in our study), 2015	OCT angiography AngioAnalytics†	None	135 (70), 3 age groups	48.3 ± 17.5 (20–79)	0.28 ± 0.10 mm²

Values within parentheses in final column represent the 95% confidence interval. FA, computer assisted-fluorescein angiography; Nd: no data.
* ImageJ, external software of measured areas.
† AngioAnalytics, internal software (Optovue, Inc.) for automatic border detection of foveal avascular zone.

prototype software used in this study may help to improve the concept of VD grading with high inter- and intraexaminer repeatability and interexaminer reproducibility. The results of our study could help differentiate healthy subjects from patients suffering progressive stages of various retinal vascular diseases.

Acknowledgments

Disclosure: **F. Coscas**, None; **A. Sellam**, None; **A. Glacet-Bernard**, None; **C. Jung**, None; **M. Goudot**, None; **A. Miere**, None; **E.H. Souied**, None

References

1. Buttery RG, Hinrichsen CF, Weller WL, Haight JR. How thick should a retina be? A comparative study of mammalian species with and without intraretinal vasculature. *Vision Res*. 1991;31:169–178.
2. Gariano RF, Iruela-Arispe ML, Hendrickson AE. Vascular development in primate retina: comparison of laminar plexus formation in monkey and human. *Invest Ophthalmol Vis Sci*. 1994;35:3442–3455.
3. Hughes S, Yang H, Chan-Ling T. Vascularization of the human fetal retina: roles of vasculogenesis and angiogenesis. *Invest Ophthalmol Vis Sci*. 2000;41:1217–1228.
4. Tan PE, Yu PK, Balaratnasingam C, et al. Quantitative confocal imaging of the retinal microvasculature in the human retina. *Invest Ophthalmol Vis Sci*. 2012;53:5728–5736.
5. Spaide RF, Klancnik JM Jr, Cooney MJ. Retinal vascular layers imaged by fluorescein angiography and optical coherence tomography angiography. *JAMA Ophthalmol*. 2015;133:45–50.
6. Paques M, Tadayoni R, Sercombe R, et al. Structural and hemodynamic analysis of the mouse retinal microcirculation. *Invest Ophthalmol Vis Sci*. 2003;44:4960–4967.
7. Chan-Ling TL, Halasz P, Stone J. Development of retinal vasculature in the cat: processes and mechanisms. *Curr Eye Res*. 1990;9:459–478.
8. Novotny HR, Alvis DL. A method of photographing fluorescence in circulating blood in the human retina. *Circulation*. 1961;24:82–86.
9. Jia Y, Tan O, Tokayer J, et al. Split-spectrum amplitude-decorrelation angiography with optical coherence tomography. *Opt Express*. 2012;20:4710–4725.
10. Tokayer J, Jia Y, Dhalla AH, Huang D. Blood flow velocity quantification using split-spectrum amplitude-decorrelation angiography with optical coherence tomography. *Biomed Opt Express*. 2013;4:1909–1924.
11. Choi W, Mohler KJ, Potsaid B, et al. Choriocapillaris and choroidal microvasculature imaging with ultrahigh speed OCT angiography. *PLoS One*. 2013;8:e81499.
12. Matsunaga D, Puliafito CA, Kashani AH. OCT angiography in healthy human subjects. *Ophthalmic Surg Lasers Imaging Retina*. 2014;45:510–515.
13. Coscas F, Glacet-Bernard A, Miere A, et al. Optical coherence angiography in retinal vein occlusion: evaluation of superficial and deep capillary plexuses. *Am J Ophthalmol*. 2016;161:160–171.
14. Couturier A, Mané V, Bonnin S, et al. Capillary plexus anomalies in diabetic retinopathy on optical coherence tomography angiography. *Retina*. 2015;35:2384–2391.
15. Thorell MR, Zhang Q, Huang Y, et al. Swept-source OCT angiography of macular telangiectasia type 2. *Ophthalmic Surg Lasers Imaging Retina*. 2014;45:369–380.
16. Agemy SA, Scripsema NK, Shah CM, et al. Retinal vascular perfusion density mapping using optical coherence tomography angiography in normals and diabetic retinopathy patients. *Retina*. 2015;35:2353–2363.
17. De Carlo TE, Chin AT, Bonini Filho MA, et al. Detection of microvascular changes in eyes of patients with diabetes but not clinical diabetic retinopathy using optical coherence tomography angiography. *Retina*. 2015;35:2229–2235.
18. Veverka KK, AbouChehade JE, Iezzi R Jr, Pulido JS. Noninvasive grading of radiation retinopathy: the use of optical coherence tomography angiography. *Retina*. 2015;35:2400–2410.
19. Kraus MF, Potsaid B, Mayer MA, et al. Motion correction in optical coherence tomography volumes on a per A-scan basis using orthogonal scan patterns. *Biomed Opt Express*. 2012;3:1182–1199.
20. Snodderly DM, Weinhaus RS, Choi JC. Neural-vascular relationships in central retina of macaque monkeys (Macaca fascicularis). *J Neurosci*. 1992;12:1169–1193.
21. Adhi M, Aziz S, Muhammad K, Adhi MI. Macular thickness by age and gender in healthy eyes using spectral domain optical coherence tomography. *PLoS One*. 2012;7:e37638.
22. Liu T, Hu AY, Kaines A, Yu F, Schwartz SD, Hubschman JP. A pilot study of normative data for macular thickness and volume measurements using cirrus high-definition optical coherence tomography. *Retina*. 2011;31:1944–1950.
23. Chan G, Balaratnasingam C, Yu PK, et al. Quantitative morphometry of perifoveal capillary networks in the human retina. *Invest Ophthalmol Vis Sci*. 2012;53:5502–5514.
24. Coscas GJ, Lupidi M, Coscas F, Cagini C, Souied EH. Optical coherence tomography angiography versus traditional multimodal imaging in assessing the activity of exudative age-related macular degeneration: a new diagnostic challenge. *Retina*. 2015;35:2219–2228.
25. Wang X, Jiang C, Ko T, et al. Correlation between optic disc perfusion and glaucomatous severity in patients with open-angle glaucoma: an optical coherence tomography angiography study. *Graefes Arch Clin Exp Ophthalmol*. 2015;253:1557–1564.
26. Freiberg FJ, Pfau M, Wons J, Wirth MA, Becker MD, Michels S. Optical coherence tomography angiography of the foveal avascular zone in diabetic retinopathy [published online ahead of print September 4, 2015]. *Graefes Arch Clin Exp Ophthalmol*.
27. Bonini F, Marco A, Adhi M, et al. Optical coherence tomography angiography in retinal artery occlusion. *Retina*. 2015;35:2339–2346.
28. Bonnin S, Mané V, Couturier A, et al. New insight into the macular deep vascular plexus imaged by optical coherence tomography angiography. *Retina*. 2015;35:2347–2352.
29. John D, Kuriakose T, Devasahayam S, Braganza A. Dimensions of the foveal avascular zone using the Heidelberg retinal angiogram-2 in normal eyes. *Indian J Ophthalmol*. 2011;59:9–11.
30. Tam J, Martin JA, Roorda A. Noninvasive visualization and analysis of parafoveal capillaries in humans. *Invest Ophthalmol Vis Sci*. 2010;51:1691–1698.
31. Kim DY, Fingler J, Zawadzki RJ, et al. Noninvasive imaging of the foveal avascular zone with high-speed phase-variance optical coherence tomography. *Invest Ophthalmol Vis Sci*. 2012;53:85–92.
32. Chui TY, Vannasdale DA, Elsner AE, Burns SA. The association between the foveal avascular zone and retinal thickness. *Invest Ophthalmol Vis Sci*. 2014;55:6870–6877.
33. Bresnick GH, Condit R, Syrjala S, et al. Abnormalities of the foveal avascular zone in diabetic retinopathy. *Arch Ophthalmol*. 1984;102:1286–1293.

34. Arend O, Wolf S, Harris A, et al. The relationship of macular microcirculation to visual acuity in diabetic patients. *Arch Ophthalmol*. 1995;113:610–614.
35. Carpineto P, Mastropasqua R, Marchini G, et al. Reproducibility and repeatability of foveal avascular zone measurements in healthy subjects by optical coherence tomography angiography. *Br J Ophthalmol*. 2016;100:671–676.
36. Takase N, Nozaki M, Kato A, Ozeki H, Yoshida M, Ogura Y. Enlargement of foveal avascular zone in diabetic eyes evaluated by en face optical coherence tomography angiography. *Retina*. 2015;35:2377–2383.
37. Samara WA, Say EA, Khoo CT, et al. Correlation of foveal avascular zone size with foveal morphology in normal eyes using optical coherence tomography angiography. *Retina*. 2015;35:2188–2195.
38. Kuehlewein L, Tepelus TC, An L, et al. Noninvasive visualization and analysis of the human parafoveal capillary network using swept source OCT optical microangiography. *Invest Ophthalmol Vis Sci*. 2015;56:3984–3988.
39. Bird AC, Weale RA. On the retinal vasculature of the human fovea. *Exp Eye Res*. 1974;19:409–417.
40. Hayreh SS. In vivo choroidal circulation and its watershed zones. *Eye (Lond)*. 1990;4(pt 2):273–289.
41. Spaide RF, Fujimoto JG, Waheed NK. Image artifacts in optical coherence tomography angiography. *Retina*. 2015;35:2163–2180.
42. Jia Y, Bailey S, Hwang T, et al. Quantitative optical coherence tomography angiography of vascular abnormalities in the living human eye. *Proc Natl Acad Sci U S A*. 2015;112:E2395–E2402.
43. Gadde SG, Anegondi N, Bhanushali D, et al. Quantification of vascular density in retinal optical coherence tomography angiography images using local fractal dimension. *Invest Ophthalmol Vis Sci*. 2016;57:246–252.

Investigative Ophthalmology & Visual Science